Available online at www.sciencedirect.com
SCIENCE DIRECT®
Journal of Molecular Catalysis A: Chemical 216 (2004) 67–74
JOURNAL OF MOLECULAR CATALYSIS A: CHEMICAL
www.elsevier.com/locate/molcata

Structure and reaction studies on vanadium molybdenum mixed oxides

Andreas H. Adams [a,*], Frank Haaß [a], Thorsten Buhrmester [a], Jan Kunert [b], Jörg Ott [b], Herbert Vogel [b], Hartmut Fuess [a]

[a] *Institute for Materials Science, TU Darmstadt, Petersenstrasse 23, D-64287 Darmstadt, Germany*
[b] *TU Darmstadt, Ernst–Berl-Institute of Technical and Macromolecular Chemistry, Petersenstrasse 20, D-64287 Darmstadt, Germany*

Received 12 December 2003; received in revised form 16 January 2004; accepted 5 February 2004

Available online 9 April 2004

Abstract

Vanadium molybdenum mixed oxides are used for the technical production of acrylic acid by partial oxidation of acrolein. Although this industrial process is established since several years, the catalytic mechanism is not known in detail. For an improved understanding of the reaction on a microscopic scale, we used subsystems such as V–Mo-oxides without additional promoters as model catalyst.

Three series of mixed oxides with the chemical composition $V_xMo_yO_z$, $x + y = 1$, were prepared; one by melting the pure oxides, one by crystallisation and another by spray-drying of ammonium salt precursors and subsequent calcination. The phases were analysed by X-ray diffraction. Most of the samples consist of two different vanadium molybdenum mixed oxides, a hexagonal h-$(V,Mo)O_3$ and a $(V,Mo)_2O_5$-phase, which is structurally related to vanadium pentoxide. The stability and the transformation of these phases were also examined. The selectivity and conversion rate for the partial oxidation of acrolein to acrylic acid was determined by temperature programmed reduction (TPR) to optimise the vanadium molybdenum ratio for an efficient catalytic phase. The results indicate a vanadium to molybdenum ratio of 3:7 as the most promising with respect to selectivity and activity at low temperatures.

Keywords: Vanadium molybdenum oxides; Heterogeneous catalysis; Acrolein; XRD; TPR

1. Introduction

The V–Mo–O system was chosen to determine the relation of structure and catalytic selectivity. As an example the production of acrylic acid by partial oxidation of acrolein is selected. This process is well understood on a macroscopic scale [1], and kinetic measurements indicate that the reaction can be described by the *Mars-van-Krevelen* mechanism proposed almost 50 years ago [2].

In contrast, on a microscopic scale, the single steps of the mechanism are not known in detail, and not even the catalytic active phase(s) or site(s) have been identified unambiguously.

In previous works different oxide species are reported to be part of the active phase system in these catalysts. Andrushkevich [3] revealed MoO_3 and V_2O_4 as major components of the V–Mo–O-catalysts and reported that the catalytic activity is related to the content of V^{4+}. Tichy et al. [4] identified VMo_3O_{11}, whereas Schlögl and coworkers [5] have proposed VMo_4O_{14} as active phase. Both mixed oxides build layer structures, belonging to the shear structures. Schlögl and coworkers [5] explain that these structures are able to integrate and remove oxygen by a transition from corner linked octahedra into edge sharing regions. Also pure vanadiumpentoxide is used as catalyst in industrial processes, a common example is the production of sulphuric acid.

To determine the catalytically active phases and the conditions of their formation and transformation samples are prepared differently. One mixed oxide series was fused from the metal oxides, vanadium pentoxide and molybdenum trioxide, in order to explore the thermodynamic stable phases. Two other sample series were prepared by crystallisation or spray-drying from the ammonium salt solution followed by a calcination step, a common way to prepare catalysts for industrial use. In the mixed oxide system under investigation the vanadium to molybdenum ratio was varied over the complete composition range. Phase analysis by X-ray diffraction was carried out for every sample as well as a characterisation by temperature programmed reduction (TPR).

* Corresponding author. Tel.: +49-6151-166355; fax: +49-6151-166023.
E-mail address: aadams@tu-darmstadt.de (A.H. Adams).

1381-1169/$ – see front matter © 2004 Elsevier B.V. All rights reserved.
doi:10.1016/j.molcata.2004.02.005

2. Experimental

2.1. Sample preparation

Three groups of samples prepared by different routes were examined. In this paper the sample composition is always given by $V_xMo_yO_z$, with $x+y=1$; $z=2.5x+3y$. Oxygen defects are assumed but not taken into account.

The first group of samples was prepared by a combination of liquid and solid phase reaction (group 1). Mixtures of the pure oxides V_2O_5 (Alfa Aesar, >99.995%) and MoO_3 (Alfa Aesar, >99.998%) were fused in the desired composition at 800 °C in a sealed silica ampoule to obtain a homogeneous oxide mixture. After pulverisation in an agate mortar, the brown to black powders were pelletised and equilibrated on an alumina plate in air at 600 °C for 7 days. The pellets were then quenched in liquid nitrogen to retain equilibrium. In each case, the sample stoichiometry was controlled by X-ray fluorenscence (XRF), with an accuracy of 3%. This preparation method is superior to the classic solid state reaction which needs about several weeks to reach the thermodynamic equilibrium because of the relatively slow interdiffusion process. Furthermore, due to the short period of reaction, no impurities of silica or alumina could be detected by the XRF or EDX measurements performed after the reaction.

2.1.1. Preparation via aqueous solution

The second and third group of catalysts were prepared from precursors obtained from aqueous solutions of the metal ammonium salts. Both ammonium heptamolybdate (Fluka) and ammonium metavanadate (Fluka) were mixed and dissolved in water (250 ml per 10 g of solid). Subsequently, the pH-value was adjusted to five by adding appropriate amounts of nitric acid. The solution is stirred under reflux for 90 min at 80–90 °C. The final precursor solution is split into two equal portions. One is spray-dried, the other is "dried" via crystallisation.

2.1.1.1. Precursor formation by spray-drying (group 2). The spray-drying process was performed in a self-constructed apparatus. The constant volume flow (12 ml min^{-1}) of the solution is pumped into the two-phase nozzle of the spray unit. Atomising is performed with compressed air at 6 bar. The resulting aerosol is dried with hot air at 270 °C. The temperature of the dried powder should not exceed 75 °C. The discharged precursor powder is directly used for characterisation and for calcination, respectively.

2.1.1.2. Precursor formation by crystallisation. The solution is partly evaporated using a rotary evaporator at 60 °C and 200 mbar. Just before crystallisation starts the process is terminated. The concentrated solution is left for crystallisation in a drying cabinet at 50 °C and at 600–800 mbar. The dried precursor is ground in a mortar. This precursor powder is directly used for characterisation and for calcination, respectively.

2.1.1.3. Calcination. The solid precursor powder was calcinated under nitrogen flux in a self-constructed calcination furnace. The temperature program was designed semi-empirically (based on TG/DTA-MS and XRD investigations). The precursor is heated to 150 °C with a rate of 2 K min^{-1}, followed by an isothermic phase of 240 min, and then heated again to 400 °C (2 K min^{-1}), where it resides for another 110 min period and cooled to RT.

2.2. X-ray diffraction

The X-ray diffraction data of group 1 oxides were collected on a Stoe STADI-P powder diffractometer equipped with a 6° position sensitive detector (PSD) in transmission geometry. Mo $K\alpha_1$-radiation and Co $K\alpha_1$-radiation (λ(Mo $K\alpha_1$) = 0.70926 Å; λ(Co $K\alpha_1$) = 1.78892 Å; Ge(1 1 1) monochromator) were used. Samples were pulverised and fixed as a thin layer on an acetate film. With Mo-radiation the samples were measured in the range of $5^\circ \leq 2\theta \leq 40^\circ$, with Co-radiation in the interval was $5^\circ \leq 2\theta \leq 80^\circ$, with a step size of $\Delta 2\theta = 0.02^\circ$ in both cases.

For the sample groups 2 and 3 a Siemens D500 powder diffractometer (Cu Kα-radiation, λ(Cu $K\alpha_1$) = 1.54051 Å; λ(Cu $K\alpha_2$) = 1.54433 Å; pyrolytic graphite secondary monochromator) with a scintillation detector was used. On this diffractometer the data sets were collected in reflection geometry in the range of $5^\circ \leq 2\theta \leq 80^\circ$, with a step size of $\Delta 2\theta = 0.03^\circ$.

The structure refinement was carried out with the program FullProf [6] in the program package WinPLOTR according to the *Rietveld*-method [7].

For in situ X-ray diffraction measurements a high-temperature diffraction chamber HDK 2.4 (Johanna Otto GmbH) was used in combination with the Siemens D500 powder diffractometer.

2.3. TPR studies

The catalysts' performance was characterised via temperature programmed reduction (TPR) in a micro-reactor with mass spectroscopic analytics with acrolein as reducing agent. The volume fractions of the compounds acrolein, acrylic acid, carbon dioxide, and water (additionally carbon monoxide in some experiments) were monitored online.

All samples were pre-treated with 10 vol.% of oxygen in inert gas (nitrogen or argon, respectively) at 400 °C for 60 min and afterwards reduced with 5 vol.% of acrolein in inert gas with a heating rate of 10 K min^{-1}.

For a comparison of the catalysts the differential selectivity, conversion, and yield were used.

2.4. Adsorption studies (BET)

The nitrogen adsorption on the surface (BET) was determined with a Quantachrom AUTOSORB 3B with automatic data logging and evaluation. Before measurement the samples were dried at 80 °C under vacuum for about 20 h.

3. Results and discussion

3.1. Phase composition

The X-ray analysis of the group 1 samples are in a good agreement with the phase diagram by Volkov et al. [8] (cf. Fig. 1). Two vanadium molybdenum mixed oxides are described: An α-phase as a molybdenum-doped vanadium pentoxide and a β-phase given as $V_{7/3-y}Mo_{5/6-1/2y}O_8$ with $0.33 \leq y \leq 0.40$.

The results of the XRD experiments revealed the presence of the α-phase up to a molybdenum level of $y = 0.08$ with the structure of vanadium pentoxide [9]. Vanadium pentoxide crystallises in the orthorhombic system, space group *Pmmn*, with a layer structure, built up by VO_5 square pyramids sharing edges and corners. Another description is a three-dimensional network of octahedra each composed of a VO_5 square pyramid and the oxygen atom at the top of the pyramid in the next layer, as described before. EXAFS measurements at the V–K-edge ($E_0 = 5.465$ keV) and the Mo–K-edge ($E_0 = 20.000$ keV) [10] reveal statistical replacement of vanadium atoms by molybdenum atoms.

At molybdenum levels of $y \geq 0.10$ additional X-ray reflections were detected which were due to β-phase, borderline composition V_2MoO_8, as mentioned in the phase diagram determined by Volkov et al. [8].

The sample with $y = 0.40$ was determined as β-phase with a low fraction of molybdenum trioxide. The structure model of V_2MoO_8 [11] used for the refinements thus describes the β-phase very well. The structure of V_2MoO_8, monoclinic with space group *C*2, can be described as a shear structure of octahedra forming ReO_3-type slabs which are infinite in the *b* and *c* direction, but only extending over three layers of octahedra. Such slabs are joined together by octahedra with common edges.

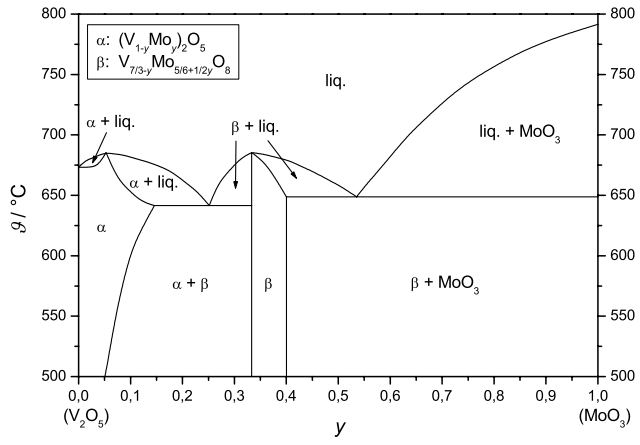

Fig. 1. Quasi-binary phase diagram of the system V_2O_5–MoO_3 (after [8]).

Above $y > 0.40$, we found a mixture of β-phase and molybdenum trioxide.

Therefore, we can conclude that the samples prepared by fusing the pure oxides are in thermodynamic equilibrium without any additional thermodynamically stable phase in the phase diagram by Volkov et al. [8].

In the vanadium-rich samples of groups 2 and 3 with $y \leq 0.2$ ($x \geq 0.8$) different vanadium oxides, mostly vanadium pentoxide, were detected, whereas in the range $y = 0.2$–0.9 ($x = 0.1$–0.8) primarily two different vanadium molybdenum mixed oxides are present. One mixed oxide, $V_{2-a}Mo_aO_5$, with $a = 0.4$–0.8, is structurally related with vanadium pentoxide and fitted as a triclinic structure, which can be described as corner sharing zigzag-chains of octahedra. Along the *b*-axis the octahedra are corner linked [12]. The second phase, rich in molybdenum, has the composition $V_bMo_{1-b}O_3$ [13], with $b = 0.1$–0.2. It crystallises in the hexagonal system, space group $P6_3$, building rings of edge and corner sharing octahedra. In both mixed oxides, the vanadium and the molybdenum atoms occupy the same crystallographic positions.

The samples with $y = 0.3$; 0.4 ($x = 0.6$; 0.7) from both preparation routes (2 and 3) only contain the $(V,Mo)_2O_5$-phase. In the crystallised samples with $y = 0.5$–0.9 ($x = 0.1$–0.5) both phases can always be found while in the spray-dried samples with $y = 0.8$–0.9 ($x = 0.1$–0.2) only the h-$(V,Mo)O_3$-phase was detected. The sample with $y = 1$ ($x = 0$) consists in both cases, crystallised and spray-dried, of molybdenum trioxide.

Fig. 2 gives an overview of the complete phase analysis of sample series 2 and 3.

In situ X-ray diffraction measurements show that these mixed oxides are only stable up to a temperature of 550 °C. Above this temperature the samples transform into the thermodynamically stable oxides molybdenum trioxide and V_2MoO_8 (β-phase). This transformation is irreversible.

Comparing structural data of the vanadium molybdenum mixed oxides in both sample series the following trends were established: In the crystallised samples the lattice constants *a* and *c* of the h-$(V,Mo)O_3$-phase as well as the volume of the unit cell of the $(V,Mo)_2O_5$-phase increase with the molybdenum content (cf. Figs. 3 and 4). In the spray-dried samples the lattice constants *a* and *c* of the h-$(V,Mo)O_3$-phase also increase with *y*, but there is a discontinuity at the borderline from the two-phase to the single-phase region (cf. Fig. 5). The volume of the unit cell of the $(V,Mo)_2O_5$-phase seems to be constant in the region $y = 0.4$–0.6 (two-phase/single-phase borderline at $y = 0.4$–0.5) (cf. Fig. 6).

We can therefore state that the technical preparation route leads to metastable mixed oxides, not present in the phase diagram. Thermodynamically stable mixed oxides, however,

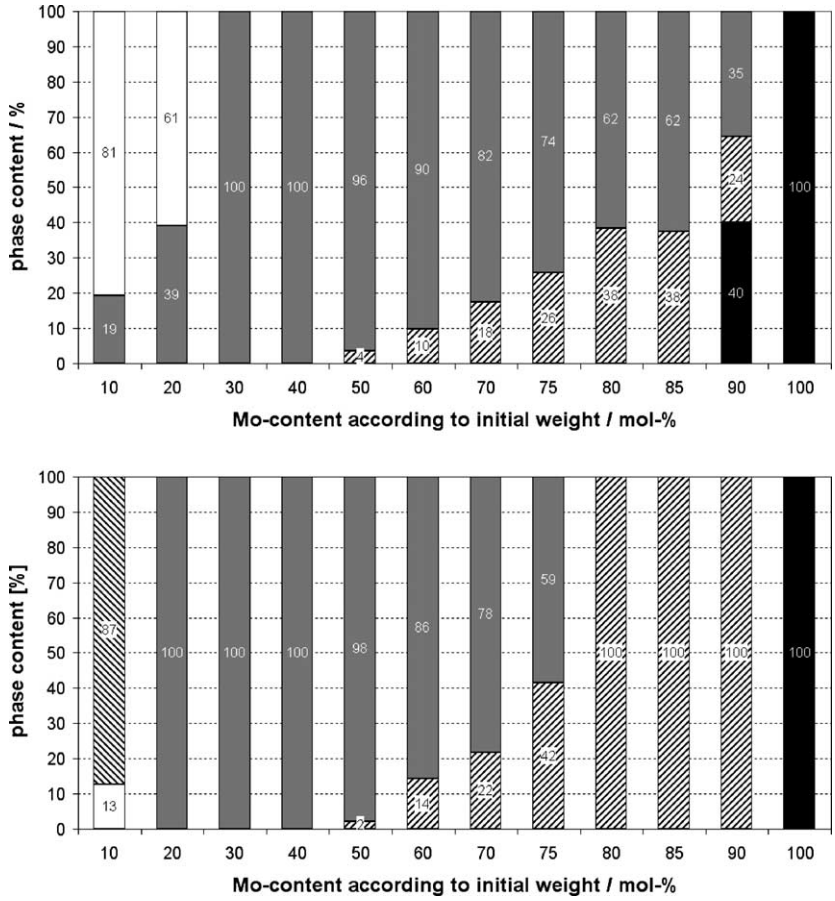

Fig. 2. Phase composition of the samples from (a) crystallised (top) and (b) spray-dried (bottom) precursors. Legend: (▨) V_6O_{13}; (□) V_2O_5; (■) $(V,Mo)_2O_5$; (▨) h-$(V,Mo)O_3$; (■) MoO_3.

prepared by fusing the pure oxides do not occur in the technical catalysts. Furthermore, there is no dramatic difference between the crystallised and the spray-dried samples.

In addition to the experiments on fresh catalysts, we examined a series of spray-dried mixed oxides, pre-treated in the micro-reactor with three cycles of acrolein/oxygen gas mixture at temperatures from 20 to 480 °C followed by a re-oxidation step at 400 °C only with oxygen in the feed. This procedure is done to eliminate the conditioning process of the catalyst, so we could do ex situ experiments on catalysts in conditioned state.

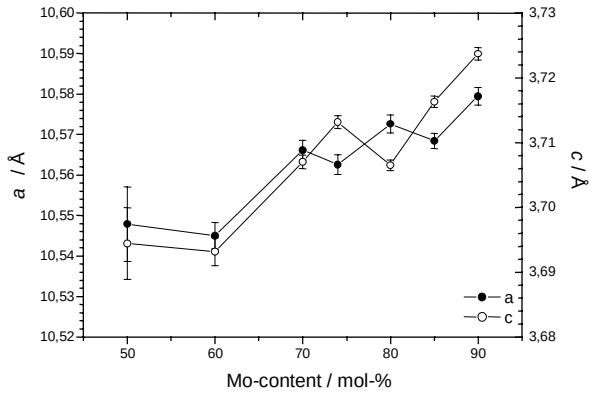

Fig. 3. Shift of the lattice constants *a* and *c* of the h-$(V,Mo)O_3$-phase in the sample series from crystallised precursors depending on the molybdenum content (with standard deviation calculated according to [14]).

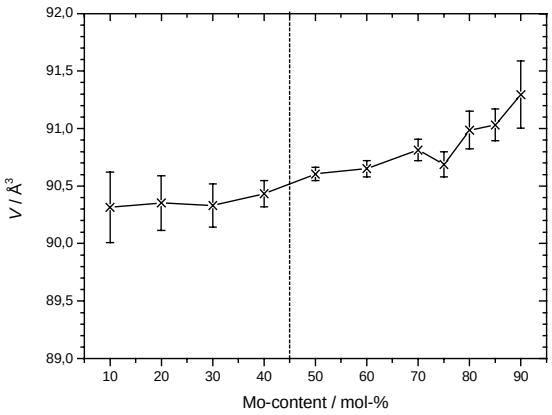

Fig. 4. Shift of the unit cell volume *V* of the $(V,Mo)_2O_5$-phase in the sample series from crystallised precursors depending on the molybdenum content (with standard deviation calculated according to [14]). The broken line marks represent the single-phase/two-phase border.

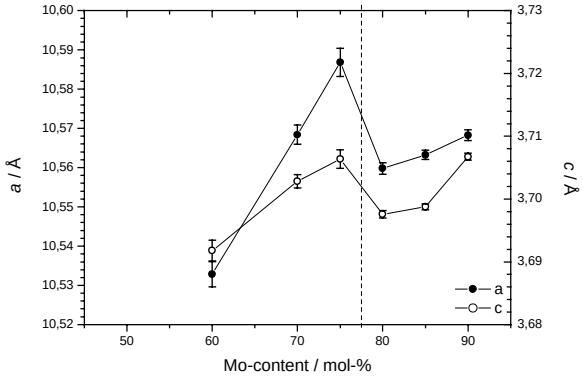

Fig. 5. Shift of the lattice constants *a* and *c* of the h-(V,Mo)O_3-phase in the sample series from spray-dried precursors depending on the molybdenum content (with standard deviation calculated according to [14]). The broken line marks represent the two-phase/single-phase border.

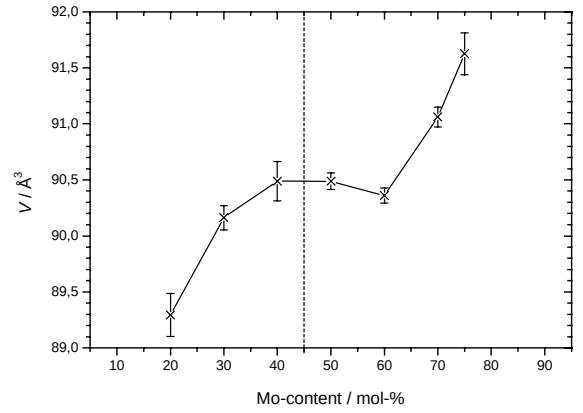

Fig. 6. Shift of the unit cell volume *V* of the (V,Mo)$_2O_5$-phase in the sample series from spray-dried precursors depending on the molybdenum content (with standard deviation calculated according to [14]). The broken line marks represent the single-phase/two-phase border.

The phase analysis of these samples shows no h-(V,Mo)O_3, therefore, molybdenum trioxide and (V,Mo)$_2O_5$ have a lager existence region according to the metal ratio of the samples (cf. Fig. 7). So we can consider that the h-(V,Mo)O_3-phase is not involved in the catalytic step. A structurally stabilising role by the formation and conditioning of the catalyst can be assumed.

3.2. In situ characterisation by temperature programmed reduction (TPR)

3.2.1. Catalysts prepared via precursor methods

All catalysts show no significant acrolein conversion at temperatures below 300 °C, therefore, a discussion of the calculated selectivity is not appropriate for this temperature range.

As a primary result, samples with a vanadium molybdenum ratio of 3:7 ($y = 0.7$) exhibited the best overall performance with a high selectivity (Figs. 8a and 9a) and significant conversion (Figs. 8b and 9b) at considerably low temperatures. With increasing vanadium fraction, the selectivity towards acrylic acid decreases, the temperature range dominated by the unselective oxidation with high acrolein conversion is extended to lower temperatures. Decreasing the vanadium fraction towards MoO_3 leads to a loss of catalytic activity.

The temperature range where the maximum selectivity and yield was observed (>450 °C) is strongly affected by the competing unselective gas phase oxidation when gas phase oxygen is present. This is the case in the industrial process of acrylic acid production, which therefore requires temperatures below 360 °C.

The differences between the samples prepared by the two different routes (Fig. 10) are negligible, a result that corresponds with the structural investigations. Quite significant

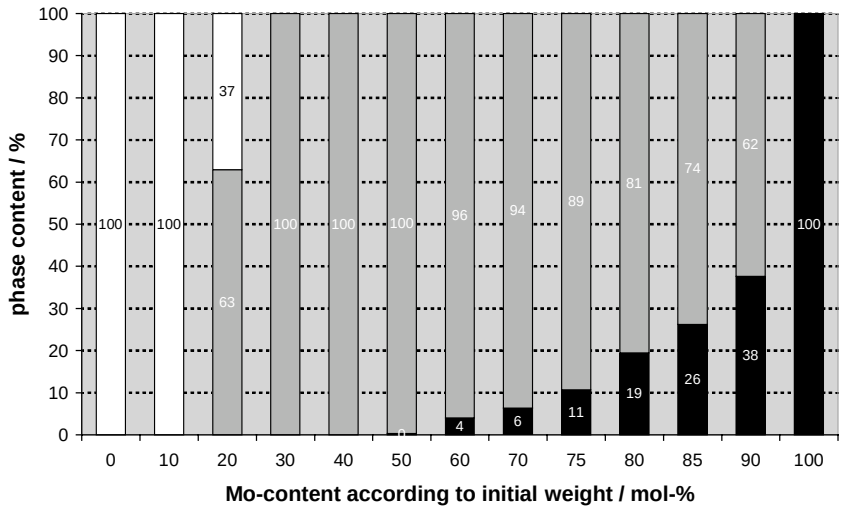

Fig. 7. Phase composition of the spray-dried catalysts pre-treated with reaction gas containing acrolein and oxygen. Legend: (□) V_2O_5; (▩) (V,Mo)$_2O_5$; (■) MoO_3.

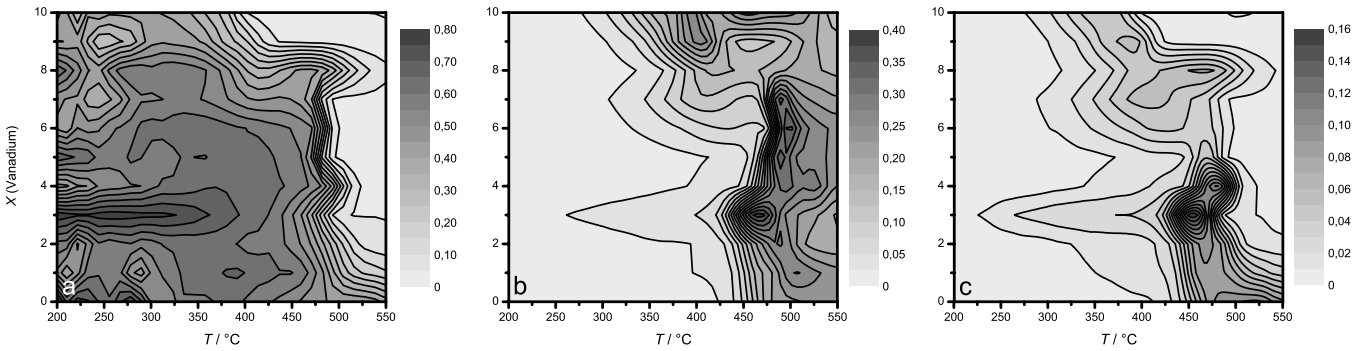

Fig. 8. Results of the TPR studies with 5% acrolein in inert gas (10 K min^{-1}) for the spray-dried sample (catalyst: $V_xMo_yO_z$; x: 10–0; y: 0–10): (a) selectivity towards acrylic acid; (b) acrolein conversion; (c) yield of acrylic acid.

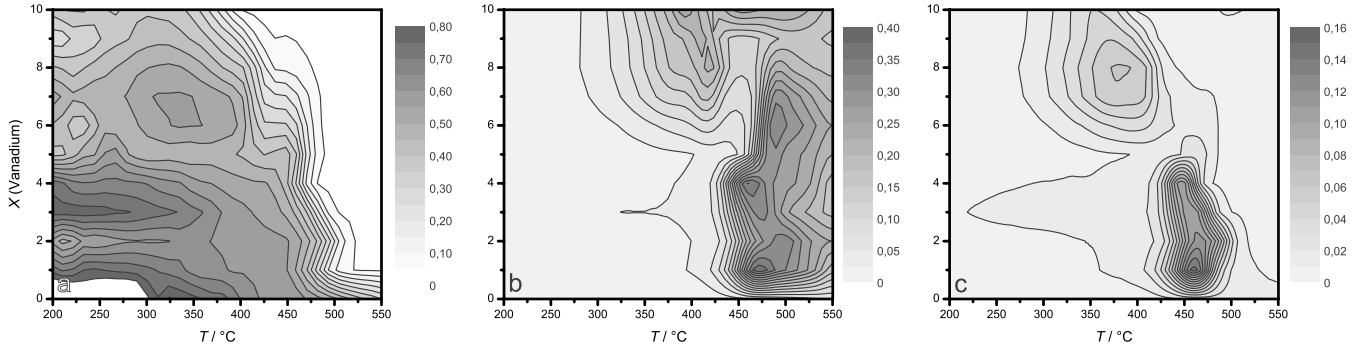

Fig. 9. Results of the TPR studies with 5% acrolein in inert gas (10 K min^{-1}) for the crystallised sample (catalyst: $V_xMo_yO_z$; x: 10–0; y: 0–10): (a) selectivity towards acrylic acid; (b) acrolein conversion; (c) yield of acrylic acid.

differences in selectivity are only observed for samples with a vanadium fraction of 40–80%, the samples prepared by crystallisation are less selective at temperatures around 470 °C.

3.2.2. Catalysts prepared via solid phase reaction

None of these catalysts showed the ability to produce a significant amount of acrylic acid, so no selectivity was calculated for these samples. Figs. 11–13 show the TPR profiles of three selected catalysts. An increase of acrolein conversion with the increasing vanadium fraction at low temperatures was observed, but for the precursor prepared catalysts the selectivity towards acrylic acid was found to be very low even for samples with V–Mo-ratio near the optimum.

3.3. Absorption studies (BET)

The nitrogen adsorption studies revealed that the samples fused out of the pure oxides and annealed for several days only have a BET surface of about 1–2 m^2 g^{-1}, while the BET surfaces of the crystallised and spray-dried samples are about a factor of 5–10 higher (cf. Table 1).

A trend depending on the metal ratio of the samples could not be established.

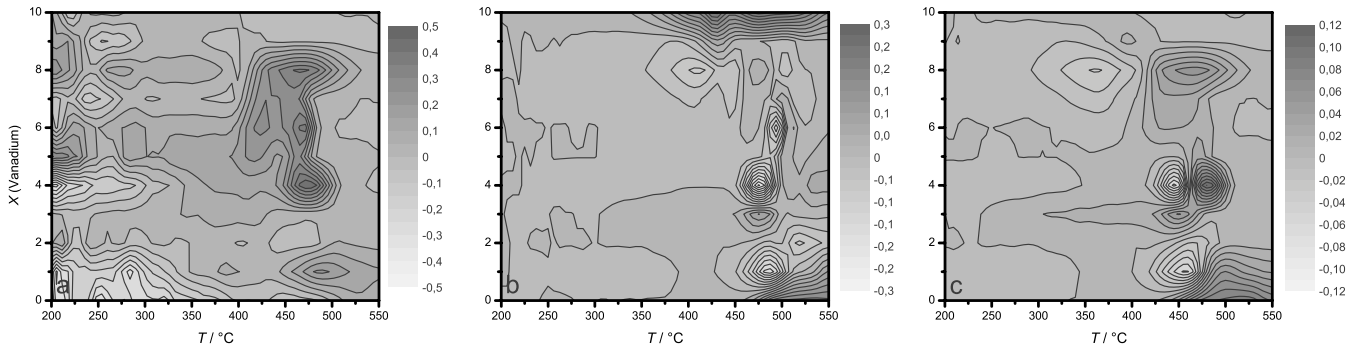

Fig. 10. Difference plot spray-dried—crystallised sample of the (a) selectivity towards acrylic acid, (b) acrolein conversion and (c) yield of acrylic acid (TPR with 5% acrolein in inert gas, 10 K min^{-1}; catalyst: $V_xMo_yO_z$; x: 10–0; y: 0–10).

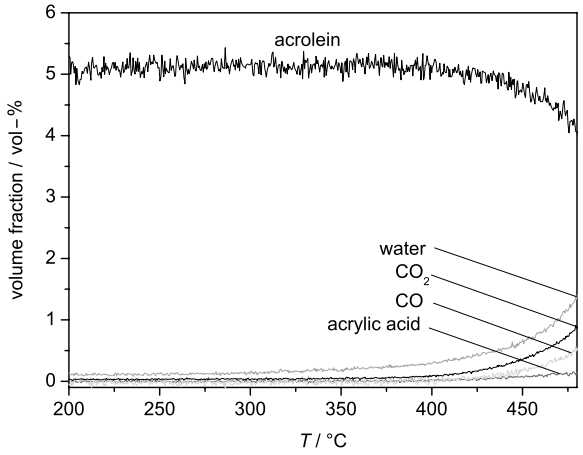

Fig. 11. Profile of the temperature programmed reduction of $V_2Mo_8O_z$, prepared via solid phase reaction, with acrolein in inert gas as reducing agent (heating rate: 10 K min^{-1}).

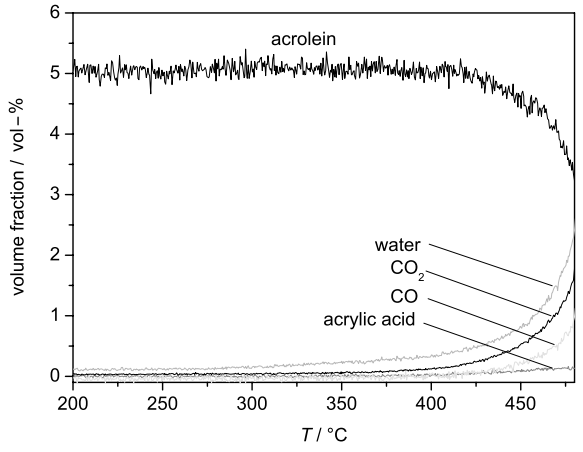

Fig. 12. Profile of the temperature programmed reduction of $V_4Mo_6O_z$, prepared via solid phase reaction, with acrolein in inert gas as reducing agent (heating rate: 10 K min^{-1}).

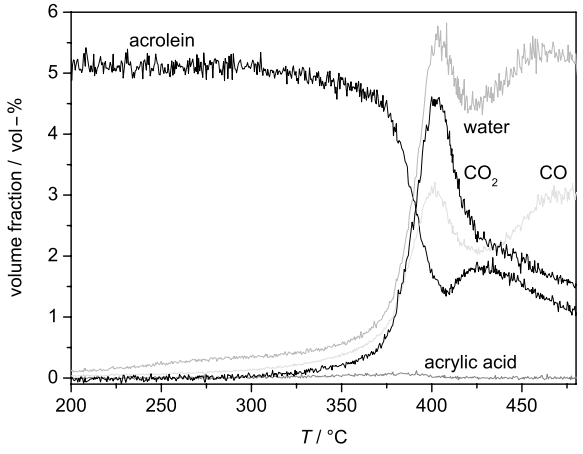

Fig. 13. Profile of the temperature programmed reduction of $V_8Mo_2O_z$, prepared via solid phase reaction, with acrolein in inert gas as reducing agent (heating rate: 10 K min^{-1}).

Table 1
BET surfaces (given in m^2 g^{-1}) depending on the metal ratio and the preparation route (with standard deviation)

Sample composition		Preparation route		
V content x	Mo content y	Solid state reaction	Crystallisation	Spray-drying
0.0	1.0	0.27 ± 0.09	2.56 ± 0.82	1.17 ± 0.37
0.1	0.9	1.31 ± 0.42	4.08 ± 1.31	2.41 ± 0.77
0.2	0.8	1.10 ± 0.35	14.53 ± 2.05	7.61 ± 2.44
0.3	0.7	1.42 ± 0.45	6.42 ± 2.05	6.76 ± 2.16
0.4	0.6	1.64 ± 0.52	11.26 ± 3,60	4.77 ± 1.53
0.5	0.5	1.73 ± 0.55	9.56 ± 3.06	6.82 ± 2.18
0.6	0.4	0.73 ± 0.23	7.80 ± 2.50	3.22 ± 1.03
0.7	0.3	1.47 ± 0.47	8.94 ± 2.86	3.87 ± 1,24
0.8	0.2	1.78 ± 0.57	8.68 ± 2,78	2.31 ± 0.74
0.9	0.1	3.43 ± 1.10	9.41 ± 3.01	5.38 ± 1.72

4. Conclusions

Our experiments showed that the preparation route of fusing the pure oxides lead to thermodynamically stable mixed oxides, which do not produce a significant amount of acrylic acid for acrolein.

The catalysts prepared by the precursor route consist primarily of two different vanadium molybdenum mixed oxides, a hexagonal h-$(V,Mo)O_3$ and $(V,Mo)_2O_5$, which is structurally related with vanadium pentoxide. The TPR-measurements with 5% acrolein in inert gas as reducing argent reveal an optimal selectivity of acrylic acid for a vanadium molybdenum ratio of 3:7. Phase analyses of catalysts, pre-treated with acrolein and oxygen in three reaction–reoxidation cycles, indicate a phase-transformation during the conditioning from h-$(V,Mo)O_3$ to $(V,Mo)_2O_5$ and MoO_3. As the production of acrylic acid by the catalysts consisting only of $(V,Mo)_2O_5$ in initial state is not as high as that at $y = 0.7$, we can conclude that the presence of h-$(V,Mo)O_3$ during the conditioning step is important for the formation of active phases. But concerning the low selectivity and activity of the examined vanadium molybdenum oxide system, we assume, that a third metal component is necessary for an efficient catalyst.

The decomposition of the catalysts into thermodynamically stable phases which have no significant catalytic selectivity for the formation of acrylic acid at temperatures higher than 500 °C is clearly shown by in situ X-ray measurements and confirmed by TPR-experiments.

Acknowledgements

The authors would like to thank Dr. H. Ehrenberg and Dr. A. Drochner (TU Darmstadt) for helpful discussions. Financial support by the Deutsche Forschungsgemeinschaft DFG, SPP 1091, and the Fonds der Chemischen Industrie is gratefully acknowledged.

References

[1] K. Krauß, A. Drochner, M. Fehlings, J. Kunert, H. Vogel, J. Mol. Catal. A: Chem. 177 (2002) 237–245.
[2] P. Mars, D.W. van Krevelen, Chem. Eng. Sci. 3 (1954) 41–59 (special supplement).
[3] T.V. Andrushkevich, Catal. Rev.-Sci. Eng. 35 (1993) 213–259.
[4] J. Tichy, J. Svachula, J. Farbotko, J. Goralski, T. Paryjcak, Czech. Nauk. Politech. Lodz. Chem. 616 (1991) 95–105.
[5] H. Werner, O. Timpe, D. Herein, Y. Uchida, N. Pfänder, U. Wild, R. Schlögl, Catal. Lett. 44 (1997) 153–163.
[6] J. Rodriguez-Carvajal, Abstracts of the Satellite Meeting on Powder Diffraction on the XV. Congress of the IUCr, Toulouse, 1990, p. 127.
[7] L.B. McCusker, R.B. Von Dreele, D.E. Cox, D. Louër, P. Scardi, J. Appl. Cryst. 32 (1999) 36–50.
[8] V.L. Volkov, G.Sh. Tynkacheva, A.A. Fotiev, E.V. Tkachenko, Russ. J. Inorg. Chem. 17 (1972) 1469–1470.
[9] R. Enjalbert, J. Galy, Acta Cryst. C 42 (1986) 1467–1469.
[10] F. Haaß, A.H. Adams, G. Schimanke, T. Buhrmester, M. Martin, H. Fuess, Phys. Chem. Chem. Phys. 5 (2003) 4317–4324.
[11] H.A. Eick, L. Kihlborg, Acta Chem. Scand. 20 (1966) 1658–1666.
[12] L.M. Plyasova, L.P. Solov'eva, G.N. Kryukova, V.A. Zabolotnyi, I.P. Olen'kova, Zh. Strukt. Khim. 32 (1991) 110–115.
[13] Y.-T. Hu, P.K. Davies, J. Solid State Chem. 105 (1993) 489–503.
[14] J.-F. Bérar, P. Lelann, J. Appl. Cryst. 24 (1991) 1–5.